

An Updated Mineralogical Analysis of Sediment Materials from Three Therapeutically-used Peruvian Lagoons

María Luisa CERON LOAYZA^{1*}, Jorge Aurelio BRAVO CABREJOS¹,
F. A. R. NAVARRO¹ and Franco URCIA CHAVEZ^{1,2}

¹ Facultad de Ciencias Físicas. Universidad Nacional Mayor de San Marcos (UNMSM), Av. Germán Amézaga s/n, Lima 01, Peru.

² Universidad Nacional Pedro Ruiz Gallo (UNPRG), Calle Juan XXIII No 391, Lambayeque, Peru.

Abstract

Herein, we determine the elemental, structural and mineralogical characterization of samples collected in three Peruvian lagoons; likewise, we investigate the physical and chemical properties of their fractions, both clay and magnetic. These lagoons are located in the Chilca District, Cañete Province, southern Lima Region, Peru; their morphology has been altered since we carried out a previous study five years ago. The physical analytical techniques used were energy dispersive X-ray fluorescence (EDXRF); X-ray diffractometry (XRD); and transmission Mössbauer spectroscopy (TMS), at room and liquid-helium temperatures, and at low and high velocities. The results indicate that dolomite is the main clayey phase presenting structural sites occupied by Fe²⁺ and Fe³⁺ cations; the mineralogy of the magnetic fraction shows the presence of hematite and magnetite

Keyword: Sediments; Medicinal mineral waters; Energy dispersive X-ray fluorescence; X-ray diffractometry; Transmission Mössbauer spectroscopy.

DOI: 10.14456/jmmm.2015.7

Introduction

We introduce recent results of the study of sediment samples that were collected in three Peruvian lagoons. They are known as follows: "La Milagrosa", "La Mellicera" and "La Encantada" (three Spanish expressions standing for "The Miraculous", "The Twin Maker", and "The Enchanted", respectively). They are located in the Chilca District, Cañete Province, Peru. Studies concerning lagoons and ponds having medicinal mud exist for long in the scientific literature. For instance, Fouret *et al.* 1996a, 1996b; Herrera *et al.* 1996; Gomes *et al.* 2013. Now, more specifically, earlier reportedly researches about the lagoons of Chilca are in Cerón Loayza *et al.* 1996, and Cerón Loayza & Mejía Santillán 2010. We are motivated to update the investigations because the lagoons of Chilca could have been disturbed by the construction of a thermal power station. At the moment, the Chilca district constitutes a Peruvian national energy center. There are currently five thermal power stations,

namely, Enersur, Kallpa, Termochilca, Duke Energy and Fenix Power; the last-named is located close to the lagoons. All of these stations generate almost 40% of the country's electricity

"La Milagrosa" is by far larger than the other two lagoons; it covers approximately a surface area of 10000 m², and it is surrounded by several mud puddles. "La Milagrosa" has been modified since we have observed that its waters are much shallower than nine years ago (Cerón Loayza & Mejía Santillán 2010, sic). From "La Milagrosa" we obtained sediment samples by utilizing an extractor which allowed checking and collecting them, at different sites. These samples have diverse characteristics of color, texture and composition; we have selected five of them (Table 1). In general, we have called MML any sample from this lagoon; specifically, we named them as follows: MML-VER, MML-CR, MML-PCL, MML-NEG, and MML-EXT; except MML-EXT, extracted from the narrowest part of the lagoon, all of them were extracted from the central part of the lagoon. Similarly, "La Mellicera" is the second largest lagoon; it has a surface area of about 1900 m²;

* Corresponding author Email: malucelo@hotmail.com.

from this lagoon we analyzed only one sample we labeled MELL. Furthermore, "La Encantada" is the smallest of the three lagoons; it has a surface area of approximately 560 m²; from this pond we analyzed only one sample we named MEC. For all the lagoons, the set of extractions was performed in May 2014.

Finally, we point out that, by utilizing the aforementioned physical techniques, we have obtained

results corresponding to the sand fraction (<2 mm), clay fraction (<2 μm), and magnetic fraction.

Materials and Experimental Procedures

The primary identification of the seven collected samples is shown in Table 1.

Table 1. Primary identification of the samples being analyzed

Sample code	Lagoon name	Characteristic	Depth	Color
MML- CR	La Milagrosa	Sample having organic matter and extracted from the central part of the lagoon.	~40 cm	Creamy
MML- VER			~40 cm	Greenish
MML - NEG			~40 cm	Blackish
MML- PCL			~10 cm	Leaden
MML- EXT		Sample having organic matter and extracted from the narrowest part of the lagoon.	~10 cm	Leaden
MELL	La Mellicera	Sample having organic matter and extracted from an edge of the lagoon.	~10 cm	Blackish
MEC	La Encantada	Sample having organic matter	~35 cm	Blackish

Sample preparation

The samples were prepared in the Laboratory of Soil Analysis at UNMSM. We dried them at room temperature, then ground them with a mortar, next sift them to get different grain size fractions: Sand, silt and clay. The obtaining of this last fraction was done by the sedimentation method, which delays, on average per sample, two weeks. When the sample was being very short, we repeated the procedure to get more samples and complete the minimum quantities. Namely, we wanted to fill the sample holder and thus be able to perform further analysis by several techniques. Besides, we extracted the magnetic part of some samples, such as MML-EXT, MELL and MEC, by using a magnetic stirrer and some hand magnets that allow their adherence-thus obtaining the amount needed for the respective analyses.

Physical and chemical measurements of the samples

Measuring the degree of alkalinity

The preparation of the samples for analyzing pH was carried out in the Laboratory of Soil Analysis,

UNMSM, following standards of its Laboratory Manual. We utilized an instrument pHTestr BNC/OAKTON, model 35624-10. In Table 2, we have the values of the potential of hydrogen we obtained.

Measuring the electrical conductivity

In preparing samples to measure the electrical conductivity, it was required preparing a saturated paste as well as extracting it through a process known as filter press ; in this way, we obtained an extract we then measured with an electrical conductivity meter. This allowed us to establish a rough estimate on the amount of salt contained in the samples (Table 3).

Applied physical techniques

Energy dispersive X-ray fluorescence (EDXRF)

The analysis of the elemental composition was performed by using an portable EDXRF instrument, AmpTek mark, which uses an X-ray tube with a silver target, operating at 30 kV and 50 μA. This technique allows recognizing chemical elements Z>12 (greater than magnesium). It was also determined

the qualitative, quantitative elemental composition (Table 4). The uncertainty in the measurement of concentrations is about 10%.

X-ray diffractometry (XRD)

For a structural analysis of the minerals present in the samples, the technique of X-ray diffractometry was employed, by using a Bruker diffractometer, model D8-Focus, with a Cu-K α radiation ($\lambda = 1.54178 \text{ \AA}$), at 40 kV and 40 mA, in a vertical goniometer. The angle scale interval was $4^\circ < 2\theta < 70^\circ$ and the 2θ advance was $0.02^\circ/\text{step}$ with an interval of $3\text{s}/\text{step}$

^{57}Fe Transmission Mössbauer spectroscopy (TMS)

We used TMS to obtain detailed information on the minerals containing iron. We manipulated a conventional spectrometer having 1024 channels and using a modulation and velocity signal characterized

as being sinusoidal. The Mössbauer spectra were taken at room temperature (RT~298 K) in a transmission geometry using a Co57 source in an Rh matrix; the spectra were analyzed by using the NORMOS program (Brand 1995) in the Archaeometry Laboratory, Faculty of Physical Sciences, UNMSM

Results and Discussion

Table 2 records the results obtained from the measurements of the degree of alkalinity of the samples, and Table 3 reports results of the electric conductivity. These were recorded in situ, at the time of extracting the samples, and ex situ, in laboratory three days afterwards. All of the samples show a high degree of alkalinity, due to the high concentration of basic ions presenting in the samples

Table 2. Measurements of the potential of hydrogen

Sample code	Lagoon name	pH (in laboratory)	Temp. of the liquid (°C)
MML- CR	La Mellicera	8.60	20.90
MML- VER	La Mellicera	8.70	20.00
MML - NEG	La Mellicera	8.50	21.30
MML- PCL	La Mellicera	9.34	21.30
MML- EXT	La Mellicera	9.80	22.10
MEC	La Encantada	9.43	21.20
MELL	La Milagrosa	9.91	22.30

Table 3. Measurements of the electrical conductivity (EC)

Sample code	Lagoon name	EC (μS)	Temp. of the liquid (°C)
MML- CR	La Mellicera	182.70	21.60
MML- VER	La Mellicera	1388.00	18.80
MML - NEG	La Mellicera	1415.00	18.70
MML- PCL	La Mellicera	1180.00	20.00
MML- EXT	La Mellicera	1577.00	18.90
MEC	La Encantada	155.90	19.00
MELL	La Milagrosa	182.70	21.60

Energy dispersive X-ray fluorescence (EDXRF)

In Table 4, we compare the percentages of element presenting in each sample. The major percentages are as follows: Al, in MML-PCL; Si, in MML-EXT; S, in MML-PCL; Cl, in MML-PCL; K is almost invariant concerning any other sample;

Ca, in MML-CR; and Fe, in MML-EXT. The MML-EXT sample has more concentration of Si and Fe; MML-PCL has a larger amount of S and Cl, followed by Fe and Si. These samples are the most representative of the MML samples.

Table 4. For the samples extracted, a quantitative analysis by EDXRF: percentage per mass

Element	Samples			
	MML-EXT	MML-PCL	MML-VER	MML-CR
Al	0.0002	15.1734	0.0002	0.0002
Si	11.3744	2.2006	0.0000	0.0000
P	0.0000	0.0000	0.0000	0.0000
S	0.6520	1.9491	1.2551	0.7000
Cl	1.9103	10.0932	3.9749	3.2212
K	1.2964	1.5761	1.5663	1.7859
Ca	4.7555	8.8050	11.8307	14.0876
Ti	0.1670	0.0572	0.0000	0.0503
V	0.0000	0.0000	0.0000	0.0000
Cr	0.0092	0.0107	0.0000	0.0000
Mn	0.0866	0.0477	0.0171	0.0452
Fe	1.8213	1.2055	0.4364	1.0209
Co	0.0342	0.0199	0.0303	0.0583
Ni	0.0000	0.0000	0.0017	0.0000
Cu	0.0037	0.0014	0.0049	0.0052
Zn	0.0112	0.0096	0.0097	0.0098
Br	0.0028	0.0233	0.0051	0.0044
Rb	0.0000	0.0000	0.0000	0.0000
Sr	0.0988	0.2858	0.2788	0.4423
Zr	0.0045	0.0070	0.0155	0.0133

X-ray diffractometry

At the upper part of Figure 1, we have the results for the clay fraction in MML-EXT. We observe two structural phases: Quartz (Q), SiO₄, which is a primary mineral and difficult to dissolve; and dolomite (Do), CaMg(CO₃)₂, which has the largest peaks. Also, at the lower part of Figure 1, we have the results for the magnetic fraction in MML-EXT. We notice structural-phase hematite (Hem), magnetite (Mag) and quartz. The largest peak is an overlapping between hematite and magnetite, Hem+Mag, well defined in $2\theta = 35.5^\circ$. The second major peak is the mineral quartz defined in $2\theta = 26.6^\circ$. Besides, in Figure 2, we have X-ray diffractograms for the MEC sample; at the upper part, we have the one corresponding to the clay fraction. Four structural phases can be identified: quartz, albite (Alb), illite (Ill), Aluminum sodium silicate hydrate with formula NaAlSi₃O₁₀·2.25H₂O (NaAlSiHyd), and pyrite (Py); this last phase indicates the presence of a ferrous sulfate. Likewise, we observed an abundant presence of albite with its main peaks; additionally, we detected broad

peaks caused by two overlappings: Q + Ill in $2\theta = 28^\circ$, and Alb + Ill in $2\theta = 31^\circ$. In this sample, likely, there is a high percentage of mineral sulfur. Furthermore, at the lower part of Figure 2, in MEC X-ray diffractogram corresponding to the magnetic fraction, we observed four structural phases: quartz, diopside (Di), albite and tirodite (Tir) - even though the term manganocummingtonite is nowadays being used to the former tirodite, so far there is no consensus on the correct terminology (Hawthorne *et al.* 2012). The albite is present in both clay fraction and magnetic fraction; it is a sodium aluminosilicate; nonetheless, some isomorphism and/or ion-exchange may exist, having iron in their structure. In the magnetic fraction, tirodite is observed with well-defined peaks, contrasting with the X-ray diffractogram of the clay fraction of the same sample. Those peaks defined very well after using a magnetic stirrer. Finally, we emphasize in obtaining the clay fraction and magnetic fraction, whenever it was needed, we repeated and evaluated time and time again the respective analyses.

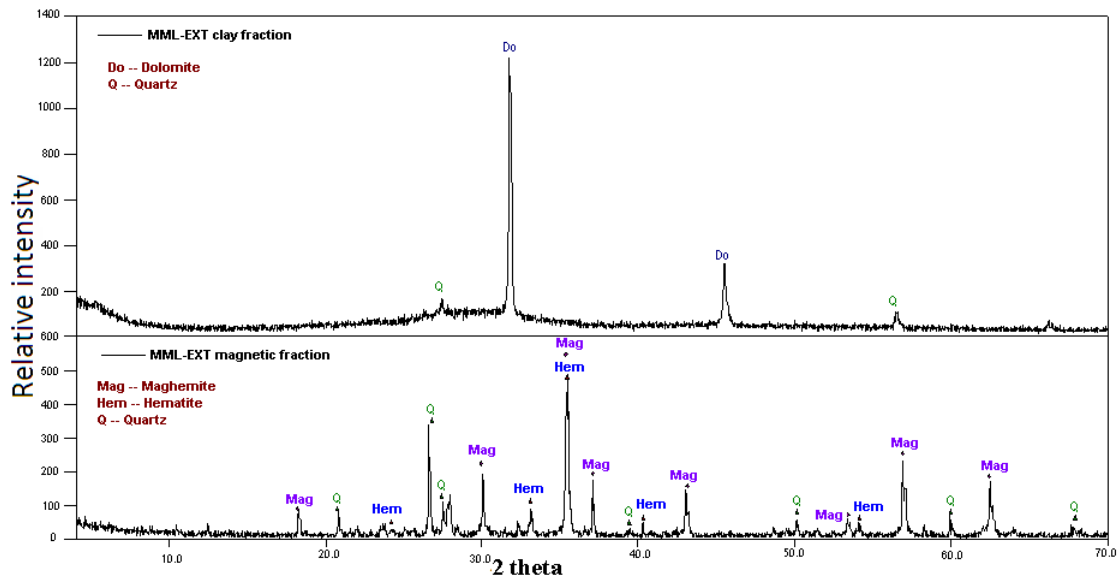


Figure 1. X-ray diffraction patterns for the MML-EXT sample. At the upper figure, we have the one corresponding to the clay fraction; at the lower figure, the one corresponding to the magnetic fraction.

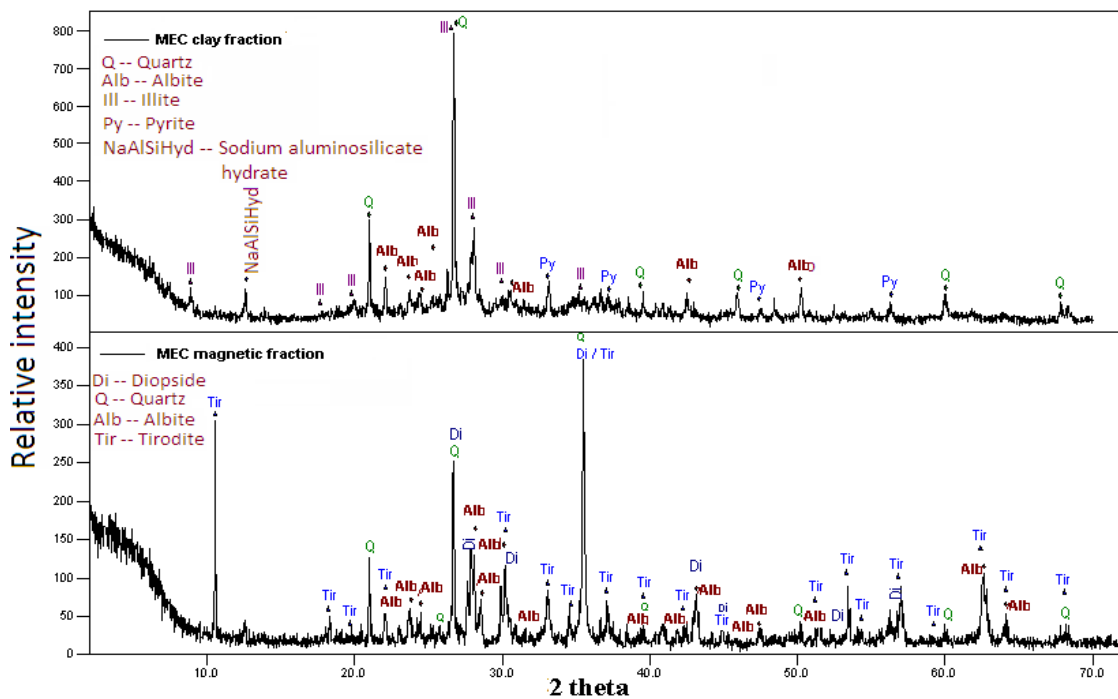


Figure 2. X-ray diffractogram for the MEC sample. At the upper figure, we have the one corresponding to the clay fraction; at the lower figure, the one corresponding to the magnetic fraction.

Transmission Mössbauer spectroscopy (TMS)

On the one hand, in Figure 3, we observed two spectra for the MML-EXT sample. On the left side, we have the one corresponding to the clay fraction, registered at low maximum Doppler velocity, $v_{max}=2\text{mm/s}$. We observed a paramagnetic contribution, which corresponds to a Fe^{3+} site, assigned to iron in dolomite with an absorption of 0.7%. On the right

side, we have the spectrum for the very MML-EXT corresponding to its magnetic fraction. The mineralogical composition is attributed to the presence of four magnetic sextets; two of them assigned to Fe^{3+} sites, corresponding to hematite; and the other two assigned to Fe^{2+} and Fe^{3+} , corresponding to magnetite. Likewise, it is noticed three paramagnetic doublets; one of them assigned to Fe^{2+} sites and the two remaining assigned to Fe^{3+} (one of them would correspond to dolomite)

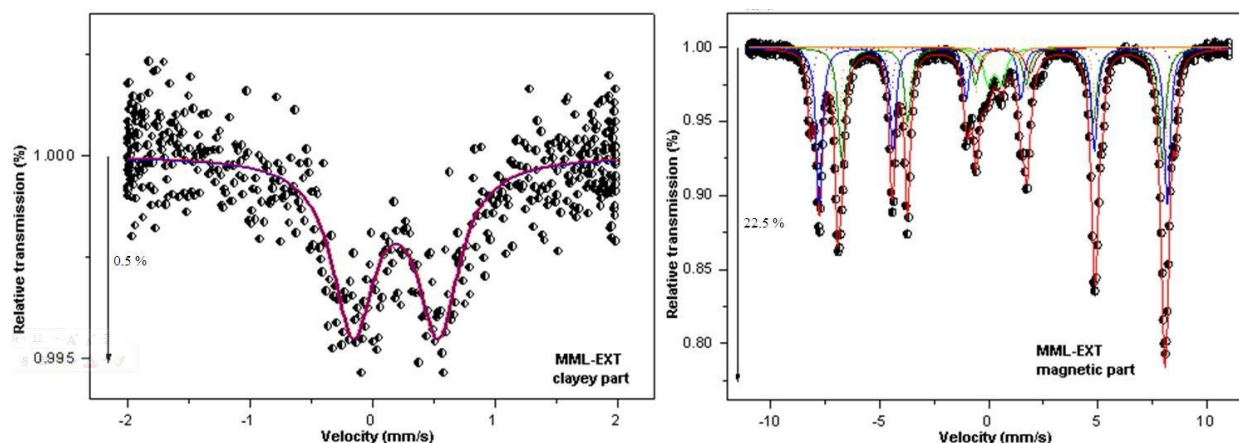


Figure 3. Transmission Mössbauer spectrum for the MML-EXT sample corresponding to the clay fraction, recorded at low maximum Doppler velocity $v_{\max} = 2$ mm/s (left side); and the one corresponding to the magnetic fraction, at velocity $v_{\max} = 11$ mm/s (right side).

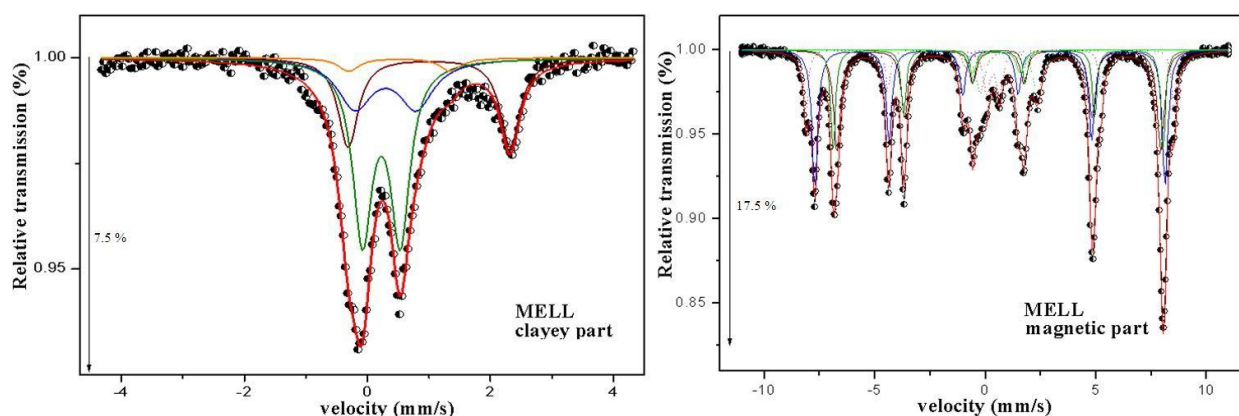


Figure 4. Transmission Mössbauer spectrum for the MELL sample corresponding to the clay fraction, recorded at low maximum Doppler velocity $v_{\max} = 4$ mm/s (left side); and the one corresponding to the magnetic fraction, at velocity $v_{\max} = 11$ mm/s. (right side).

On the other hand, in Figure 4, we observed two spectra for the MELL sample. On the left side, we have the one corresponding to the clay fraction, recorded at low speed, $v_{\max} = 2$ mm/s. We noticed four paramagnetic doublets; two of them would correspond to Fe^{3+} sites, and the other two to Fe^{2+} sites. On the right side, we have the spectrum corresponding to the magnetic fraction. The mineralogical phases are similar to those from spectra for the MML-EXT sample. This fact must be because the samples pertain to lagoons geographically very close between them; therefore, their magnetic composition must not change, even though several samples were recorded from different places of extraction.

Conclusions

Our studies of three therapeutically-used Peruvian lagoons show a high degree of alkalinity, what is caused by their high concentration of basic ions. The elemental composition has a major concentration of silicon and iron, followed by sulfur and chlorine. The dominant clay would have in its structure Fe^{2+} and Fe^{3+} sites; this clayey phase is assigned to dolomite, which has been detected by XRD and TMS techniques.

By using transmission Mössbauer spectroscopy, the mineralogy of the magnetic fraction is confirmed for two representative samples studied, what must be because the samples stem from lagoons located in the same geographical area. Thereupon, their magnetic composition did not change; it was the same for samples recorded from various places of extraction. Finally, that magnetic composition corresponds to Fe^{3+} and Fe^{2+} oxides sites, assigned to hematite as well as to magnetite.

References

1. Altman, N. (2000). *Healing Springs - The ultimate guide to taking the waters*. Healing Arts Press, Rochester, Vermont, United States of America
2. Cerón Loayza, M. L., Furet, N. R., Bravo Cabrejos, J., Bustamante Domínguez, A., Quispe Marcatoma, J., and Trujillo Quinde, A. (2005). Caracterización Mineralógica de los Peloides de Las Salinas de Chilca (Mineralogical Characterization of Peloids from Las Salinas, Chilca). *Revista de Investigación de Física, UNMSM*. **8(2)** : 9-13.
3. Cerón Loayza, M. L. and Mejía, M. (2010). Efectos del hidróxido de sodio en un tratamiento químico selectivo de peloides peruanos (Effects of sodium hydroxide in a selective chemical treatment of Peruvian peloids). *Revista de Investigación de Física*. **13(1)** : 1-4.
4. Furet, N. R., Díaz, A., Rodríguez, A. C., Portilla, C., Luna, B. and Moya, N. M. (1996). *Los Peloides de las Salinas Bidos. Un estudio por Espectroscopia Mössbauer del Fe Fe⁵⁷ y Espectrometría de Absorción Atómica* (Peloids of Bidos Salinas. A Fe⁵⁷ Mössbauer Study and Atomic Absorption Spectrometry). In: *Contribuciones a la Hidrología y Medio Ambiente en Cuba*. 341-347.
5. Furet, N. R., Rodríguez, A. C., Quintero, M. J., and Portilla C. (1996). *Evaluación Química de Peloides de Varias Salinas de Cuba* (Chemical Evaluation of Peloids of Several Cuban Salinas). In *Contribuciones a la Hidrología y Medio Ambiente en Cuba*. 349-356.
6. Gomes, C. S. F., Carretero, M. I., Pozo, M., Maraver, F., Cantista, P., Armijo, F, Legido, J. L., Teixeira, F., Rautureau, M. and Delgado, R. (2013). Peloids and Pelotherapy: Historical Evolution, Classification and Glossary. *Appl. Clay Sci.* **(75-76)** : 28-38.
7. Hawthorne, F. C., Oberti, R., Harlow, G. E., Maresch, W. V., Martin, R. F., Schumacher, J. C., and Welch, M. D. (2012). Nomenclature of the amphibole supergroup. *American Mineralogist*. **97(11-12)** : 2031-2048.
8. Herrera, I., Furet, N. R., Rodríguez, A. C., Toledo, C. and Cañizares, H. (1996). Caracterización Químico - estructural de Fangos Medicinales (Chemical and Structural Characterization of Medicinal Sludge). *Contribuciones a la Hidrología y Medio Ambiente en Cuba*. 325-339.
9. Pérez, M. and Segarte, F.R. (2001). Utilización de Recursos Termales en la Búsqueda de Salud y Belleza (Using Thermal Resources in Search of Health and Beauty). *Rev. Cubana Farm.* **35(3)** : 207-211.
10. San Martín, J. (1994). *Peloides en General. Características Físicas, Efectos Biológicos e Indicaciones Terapéuticas. Cap. 24 en Curas Balnearias y Climáticas, Talasoterapia y Helioterapia* (Peloids in General. Physical Characteristics, Biological Effects and Therapeutic indications. Chapter 24 in Spas and Climatic Cures, Thalassotherapy and Heliotherapy). Complutense, Madrid. 313-331.